EXPERIMENTAL BEAM DYNAMICS MEASUREMENTS OF NONLINEAR QUASI-INTEGRABLE LATTICES*

N. Kuklev†,1, J. Wieland[1,2], A. Romanov[1], A. Valishev[1]
[1]Fermi National Accelerator Laboratory, Batavia, IL, USA
[2]Michigan State University, East Lansing, MI, USA

Abstract

Nonlinear integrable optics is a promising design approach for suppressing fast collective instabilities. To study it experimentally, a new storage ring, the Integrable Optics Test Accelerator (IOTA), was built at Fermilab. IOTA has recently completed its fourth scientific run, achieving the design 150 MeV energy and significantly improving on various beam parameters. We present the results of beam dynamics studies of the quasi-integrable Henon-Heiles octupole system using a new equal-phase-advance spacing. We obtained tune spread and dynamic aperture scaling in agreement with tracking simulations and robust to perturbations. A new technique of direct fitting to the nonlinear lattice was developed to recover phase space dynamics, showing improved invariant jitter consistent with the intended effective Hamiltonian. We present details of the analysis and the results, and outline plans towards proton studies and a direct demonstration of reduced beam losses in the intense space charge regime.

INTRODUCTION

One of the major factors limiting peak current in circular accelerators is beam losses. Particles are lost through a variety of both coherent and incoherent (single-particle) processes - of special concern for future hadron machines are the high intensity collective effects. The standard approach to stabilize such beams is to use nonlinear elements like octupoles to produce amplitude-dependent betatron tune spread [1]. This suppresses both longitudinal and transverse instabilities by preventing resonant energy coupling to particles, and is known as Landau damping. The disadvantage of this approach is dynamic aperture reduction, again leading to beam losses [2]. A new nonlinear focusing system was proposed by Danilov and Nagaitsev (DN) [3] that is predicted to achieve significant tune spreads without such negative effects through careful shaping of the magnetic potential and special requirements on lattice optics. To test this concept, the Integrable Optics Test Accelerator (IOTA) storage ring was constructed at Fermilab [4]. We previously reported results from IOTA run 2 [5, 6], showing encouraging indicators of integrability but also significant limitations imposed by instrumentation noise, low energy, and fast signal decoherence. In this paper, we present results from run 4, which has improved on many of these aspects.

* This manuscript has been authored by FermiForward Discovery Group, LLC under Contract No. 89243024CSC000002 with the U.S. Department of Energy, Office of Science, Office of High Energy Physics.
† nkuklev@fnal.gov

INTEGRABLE OPTICS

Modern accelerator designs are based on a strong-focusing linear lattice, which has no tune spread and is fully integrable - it has the same number of conserved dynamic quantities, Courant-Snyder (CS) invariants, as degrees of freedom, and so particle motion is regular everywhere. Due to misalignments, field errors, and the need to correct chromaticity and induce tune spread, real accelerators are slightly nonlinear, and so no longer have CS invariants. Their regular motion is limited to a finite region, called the dynamic aperture (DA) - preserving DA size is critical for achieving good performance. Transverse beam dynamics are described by the Hamiltonian

$$H = \frac{1}{2}\left(K_x(s)x^2 + K_y(s)y^2 + p_x^2 + p_y^2\right) + V(x,y,s)$$

with $K_{z=x,y}$ being the linear focusing strength, and $V(x,y,s)$ containing nonlinear terms (dependent on time ($\equiv s$) and transverse (x,y) position). The DN approach is to seek solutions for V that yield two invariants and are also implementable with conventional magnets. The first invariant comes from time scaling of $V(x,y)$ to obtain a time-independent potential $U(x_N, y_N)$ in normalized CS coordinates. Then, solving for a specific transverse form of $U(x_N, y_N)$ (the DN solution) yields another invariant of motion. Such a system is both nonlinear and fully integrable. Conveniently, the first nonlinear multipole in the DN solution is an octupole, and has potential of the form

$$V(x,y,s) = \frac{\alpha}{\beta(s)^3}\left(\frac{x^4}{4} + \frac{y^4}{4} - \frac{3x^2y^2}{2}\right)$$

where $\alpha(\mathrm{m}^{-1})$ is the strength parameter. Using only this multipole produces a system of so-called Henon-Heiles type [7]. It has a single invariant of motion, and is hence only quasi-integrable (QI), with finite DA. While the QI system does not produce as large a tune spread as the DN one, even a single invariant is highly beneficial for particle stability. Moreover, QI is easily implementable with standard octupole magnets and is predicted to be significantly more robust to misalignments and other lattice errors [8]. As such, in IOTA both QI and DN systems are studied. Analysis of the invariants and dynamic aperture for the DN system was previously reported [9, 10]; this work focuses on QI analysis.

EXPERIMENTAL SETUP

IOTA is a research electron and proton storage ring recently commissioned at the Fermilab FAST facility. It is

designed to use either 2.5 MeV protons or 150 MeV electrons. The IOTA lattice is shown in Fig. 1, with an element diagram in Fig. 2 and QI insert in Fig. 3. An extensive beam diagnostics suite is available, including 21 beam position monitors (BPMs), synchrotron light cameras, DCCT, and independent vertical and horizontal single-turn kickers.

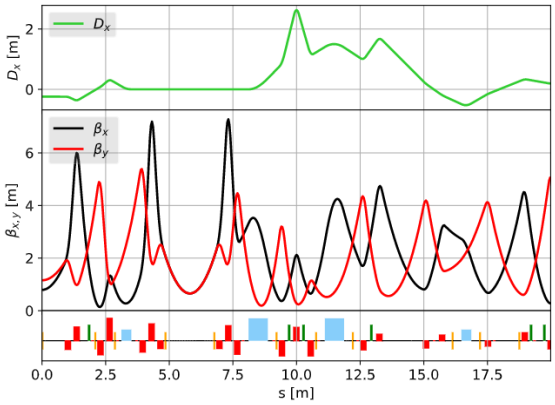

Figure 1: Half of IOTA lattice at working point $Q_{x,y}$=5.3. All units in meters, bottom - $\beta_{x,y}$, top - D_x.

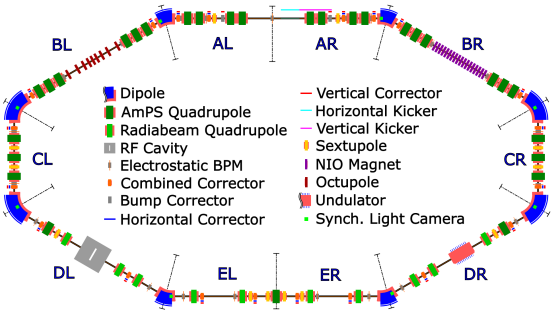

Figure 2: IOTA schematic diagram for run 4.

Even though the octupolar potential scales as $1/\beta(s)^3$ for the QI system, a new $1/\beta(s)^2$ 'equal-phase' arrangement was used for run 4 based on recent work that showed better levels of conservation if magnets are spaced according to equal linear phase between them, resembling a numeric integrator [11]. We have confirmed in simulations that a 9-magnet equal-phase layout has comparable invariant jitter to a 17-magnet equal-spacing one, both an order of magnitude lower than the naive sum of x/y Courant-Snyder invariants. In practice, the reduction in magnet count has allowed us to achieve better alignment and improve field quality by keeping the best magnets from the original 17. Power supplies were also upgraded such that the whole insert could now achieve $\pm$6A (in the central octupole, and scaled for others), delivering sufficient detuning strength at 150 MeV to ensure dynamic aperture can dominate physical aperture.

Several other hardware improvements were implemented as compared to run 2, the key one being the addition of 8 more sextupoles (from 4 previously), for a total of 6 mirror-symmetric families. This allowed for some flexibility in chromaticity correction, improving the number of observable turns before decoherence while minimizing DA degradation and unwanted nonlinear detuning contributions. A

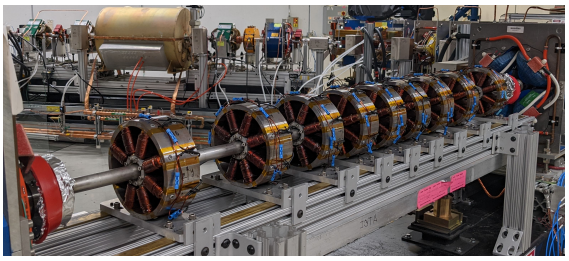

Figure 3: Octupole insert with equal-phase spacing.

dedicated Bayesian optimization study was performed to establish the 'lilac' configuration as one offering a good compromise of horizontal and vertical DA. We refer to the original SC1/SC2-only correction as the 'chromatic' sextupole config.

DATA COLLECTION AND ANALYSIS

For both the QI and DN systems, we collected TBT data after pinging the beam in X/Y parameter space for several lattice configurations and patterns (e.g. grid, spokes). At each kick with acceptable beam losses and current, arrays of 7000 turns from 21 BPMs were recorded for offline processing along with over 500 setpoints and readbacks, giving a complete snapshot of the ring state.

Preprocessing

Given the vast increase in data as compared to run 2, it was critical to implement an automated pipeline for data preprocessing and validation prior to running the analysis. We developed a veto-based set of filters both per-kick and per-BPM, including checks for too much beam loss (via DCCT or sum signal), signal asymmetry or sum jitter (indicating saturation), absence of signal (kick misfire or BPM glitch), excessive noise, and many others. A per-kick veto excluded the kick completely, while a per-BPM veto had to trigger for 2 or more BPMs. We also fully excluded BPMs A1C and E2L due to hardware issues, leaving 19 for analysis. An example kick set and per-kick vetoes are shown in Fig. 4.

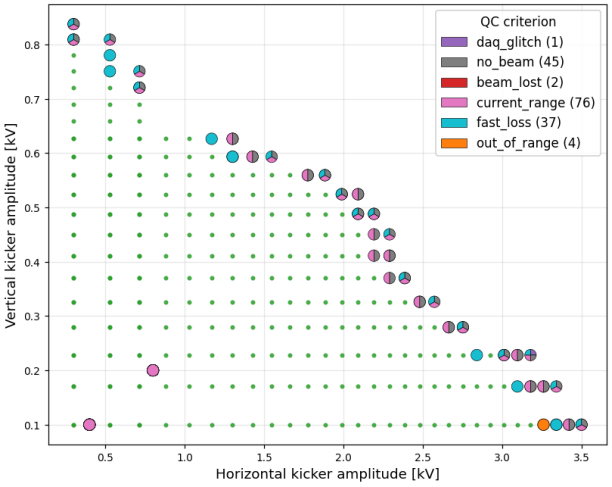

Figure 4: Quality check on a grid-type dataset.

Dynamic Apertures

A special dataset type was collected to establish the edge of dynamic aperture, consisting of 5 'spokes' aligned with 0, 22.5, 45, 67.5, and 90 degree directions in amplitude space (or alternatively defined at the center of the inserts where $\beta_x = \beta_y$ and $\alpha_x = \alpha_y = 0$). For each spoke, the beam was injected, scraped to 0.5mA, and then kicks were performed until reaching a threshold of 0.2mA. This controlled for IBS-driven beam size changes while keeping collection time reasonable. For analysis, the edge of DA was defined as the point where 25% of the beam is lost, or where 10% is lost for two consecutive kicks. If no such condition is encountered, the last kick with ≥0.25mA was considered the edge. An example spoke trace and corresponding loss fraction are shown in Fig. 5.

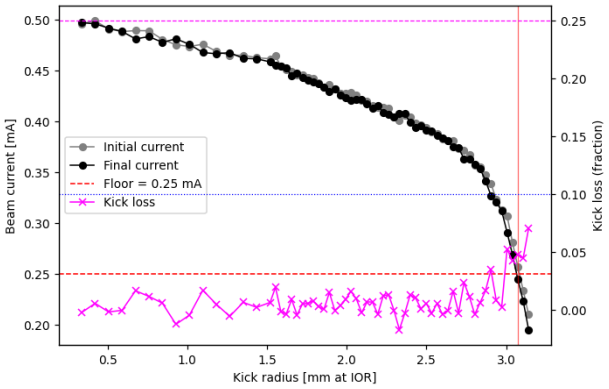

Figure 5: Current before/after and loss fraction for DA spoke. Dotted lines indicate various decision thresholds.

Tune Analysis

Data in the automatically-detected region of interest (50-150 turns) was cleaned with SVD. The strongest peaks were picked out using the NAFF algorithm [12] modified with adaptive windowing and decoherence phase correction. From the resulting set of peaks in both planes, x and y tunes were assigned according to magnitude ranking and the kick amplitudes. Because IOTA lattice has equal linear tunes, and they are not altered by the QI insert, it is very difficult to robustly discriminate tune splitting for low magnitude kicks - these are suppressed from automatic process (based on tune uncertainty), and assigned manually where possible.

Phase Space and Invariants

The phase space fitting procedure has been significantly improved to take advantage of recent developments in differentiable modeling. We use JACC (Jax for ACCelerators, [13]) to implement a fully differentiable IOTA lattice including symplectic integrators for all elements. This accounts for strong geometric nonlinearities while providing fast exact computation of the Jacobian with respect to initial coordinates. This capability is used in a custom vectorized Levenberg-Marquardt least squares fitter to perform a batch trajectory fit. Furthermore, through differentiable bunch tracking, Bayesian inference on model parameters such as bunch energy spread is possible. The impact of using nonlinear vs linear (R matrix only) models is shown in Fig. 6.

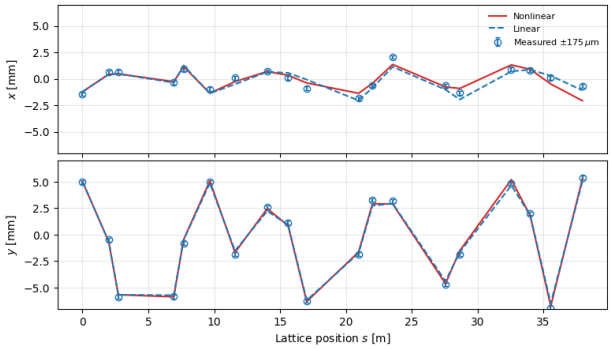

Figure 6: Fitted single turn trajectories with linear-only and full lattice models.

Strong chromatic and nonlinear decoherence is the largest challenge for invariant analysis. Instead of attempting to fit an analytical decoherence envelope [14], we limit analysis to only the first few dozen turns (depending on amplitude), which is sufficient to observe invariant jitter. All data is adjusted for BPM gains and tilts using the latest LOCO-calibrated lattice model obtained from the 6DSim utility. We also infer actions from first turn amplitudes, which accounts for the rolls in kickers and has proven more reliable than trusting the kicker setpoints. Error propagation is done using covariance matrices for the initial least squares fit, and then using Monte Carlo for further computations like invariants, including appropriate debiasing. We separately collected BPM noise calibration data without any beam kicks, finding the TBT sigma to be between 140 μm and 220 μm within the QC current range, almost identical between BPMs, meaning uniform least-squares weights could be used. For simplicity of analysis and visualization, all fits and simulations were transported back to the insert center, with limiting aperture chopped ellipse set by the DN and undulator inserts.

RESULTS

Dynamic Apertures

DA data was collected by scanning octupole current (-6A to +6A) and sextupole configuration (on, lilac, chromatic), as well as the response to perturbations in tune advance inside and outside the insert, dispersion, and location of β^* along s. Overall, we observed no more than 15% degradation in any spoke for all errors, even those several times beyond the realistic range. An example comparison for tune disturbance is shown in Fig. 7. We measured ling for both positive and negative insert currents, shown in Fig. 8, confirming the expected rate of DA degradation consistent with simulations.

Tune Footprints

The main figure of merit for NIO systems is the tune spread within the available DA. For QI, we focused on the configuration with 2 A in the central magnet to achieve an overall detuning strength at 150 MeV similar to run 2 data.

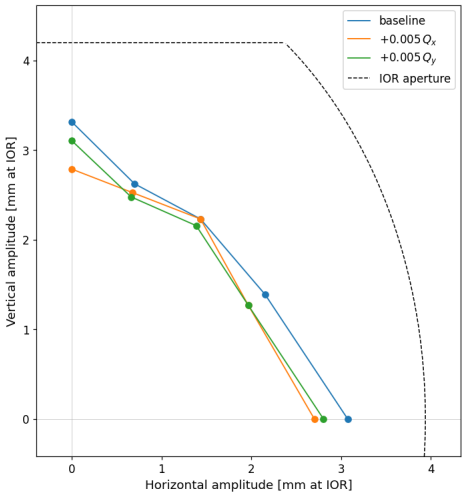

Figure 7: DA scan results for tune advance perturbations.

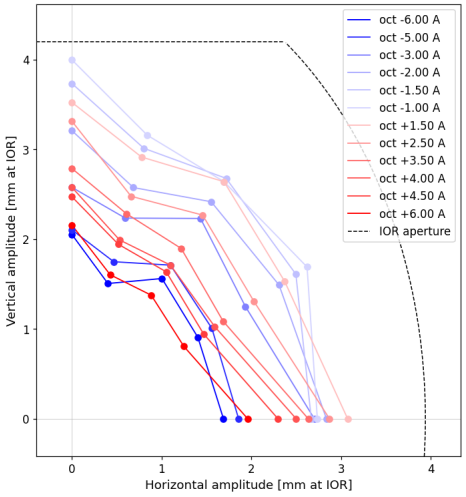

Figure 8: DA scan results for multiple QI currents.

Experimentally, this configuration showed tune shifts of $\Delta Q_{x,y} = 0.032 \pm 0.003$ in both planes, for an overall tune spread of $\Delta Q \sim 0.05$, as shown in Fig. 9. Data is in good agreement with simulations, with slight systematic offset attributed to sextupolar and soft quadrupole detuning effects.

Phase Space and Invariants

Due to concerns about soft saturation and resonances (below kick QC threshold), we selected kick strengths with at least 10% amplitude margin away from the loss edge for phase space analysis. For each kick, the first 20 turns were fitted using the previously outlined nonlinear machinery. We then computed both value and jitter estimates ($\sigma_H/\bar{H}$) and ($\sigma_I/\bar{I}$), and compared them against expected trends. Note that the strength scaling of the nonlinear Hamiltonian term was set based on design magnet gradients, which introduces some systematic calibration error for all comparisons. An example invariant recovery result for a strong vertical kick is shown in Fig. 10, and a comparison with simulations initiated at the same initial trajectory is shown in Fig. 11.

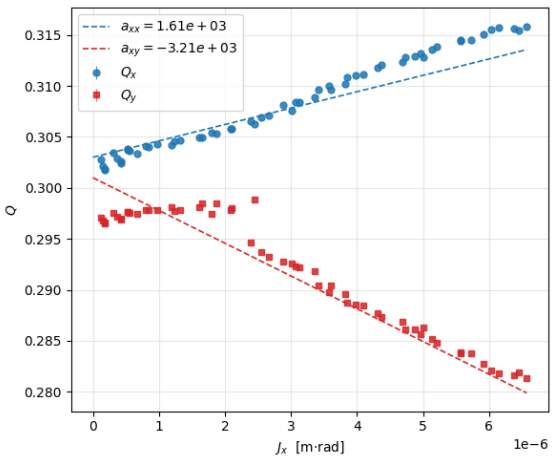

Figure 9: QI detuning along H spoke. Working point is adjusted to 0.303/0.301 based on data fit.

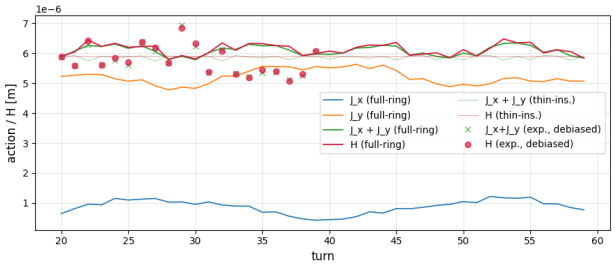

Figure 10: Invariant recovery for a single kick, in comparison to same simulation. The thin insert corresponds to ideal T-insert conditions, and has two orders of magnitude lower H jitter vs $J_x + J_y$, both are tiny on this scale.

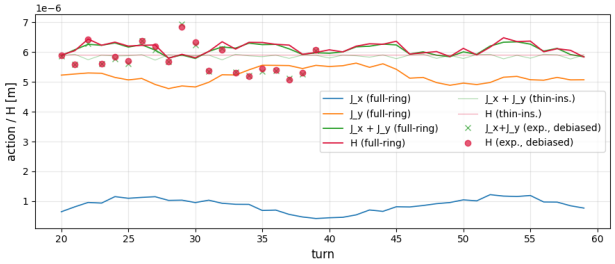

Figure 11: Invariants based on full nonlinear trajectory fit for a single representative kick.

As can be seen by the signal magnitudes, the nonlinear term is getting almost swamped by the fit uncertainty. When compared to simulation, the observed jitter is of the same order of magnitude, but the precision of the reconstruction is not sufficient to quantitatively prove better H invariant conservation. To further understand systematic and statistical errors, we collected fit quality metrics for every kick and turn, which revealed a systematic increase in residuals for higher amplitude kicks, shown in Fig. 12.

The growing discrepancy with kick amplitude might indicate that a higher order BPM/pickup distortion correction is necessary, beyond the existing 7th order polynomial (unlikely), or that the ring model has a fundamental disagreement with beam data that increases with amplitude. This

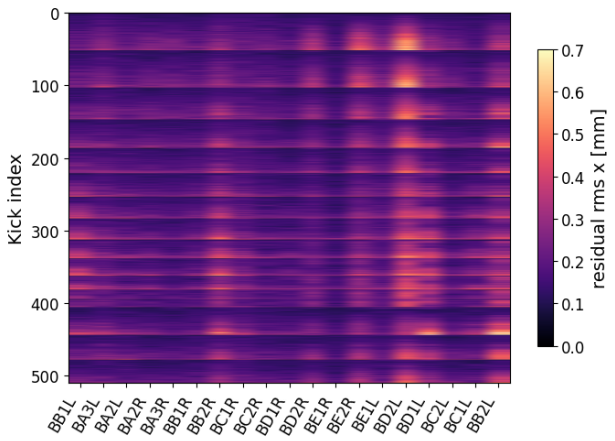

Figure 12: Residuals per turn per BPM in the x plane for a 2A QI grid dataset. Brighter lines correspond to larger errors, associated with larger kicks. The striped pattern is due to x being the inner scan dimension.

latter hypothesis is corroborated by approximately a unit difference in expected vs measured chromaticity - we are working on better field maps to refine the edge field simulations. Mean residuals, shown in Fig. 13, had fairly minor overall bias in the estimates (with exception of BPM D1L), suggesting good LOCO calibration.

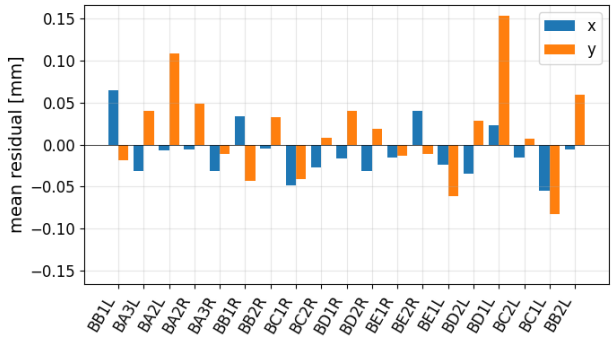

Figure 13: Mean residuals in x/y for kick set of Fig. 12.

We are reviewing the LOCO fitting as well as BPM calibration coefficients used and whether a potential misconfiguration can explain the observed D1L trends and be corrected. The overall final invariant conservation for a full kick set is shown in Fig. 14, and demonstrates very close correspondence of the CS and H values.

Over the full 2A dataset, the averaged relative jitter was 8.10% for CS vs 7.81% for H, with maxima of 11.4% vs 10.8% respectively, demonstrating a slight but statistically significant improvement for the QI system. Simulations of the full nonlinear lattice indicate that the majority of the jitter is being driven by strong sextupolar effects necessary to correct chromaticity, with the lilac configuration especially problematic for diagonal kicks once the QI system is turned on. We are continuing to improve our models of the magnetic components so as to better account for and decouple their effects from the QI contributions.

One promising general method to demonstrate the presence of invariants is the recently proposed AI Poincare [15]

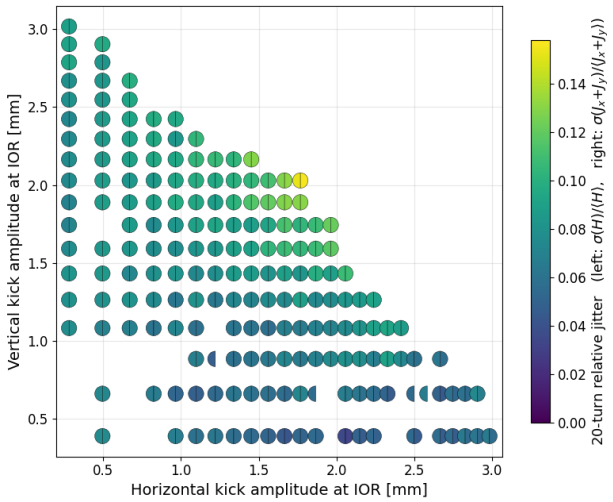

Figure 14: Jitter in CS and H invariants over 20 turns for the 2A QI grid. Where kicks disagreed by more than 20%, data was removed as indicated by a missing marker.

technique, which trains a neural network to collapse dimensions until an irreducible set has been found, corresponding to the invariants of motion. We applied it on the full nonlinear lattice simulation data, finding that sufficient confidence is obtained with around 50 turns from 12 kicks under 100 um noise to classify the QI lattice as containing 1 invariant (vs 2 for the linear lattice). This method requires careful calibration, but preliminary results from a point dataset with QI (80 kicks at an identical setpoint) are promising, demonstrating a clearly better n_{eff} as compared to an artificially spoiled configuration with 2 octupoles (which however has less data available). We are still testing overall robustness and how well this method can discriminate between configurations.

SUMMARY AND FUTURE PLANS

We have presented IOTA run 4 results for the beam dynamics studies of the QI octupole insert. The QI system was successfully rebuilt in the equal-phase configuration, and many improvements were made to the hardware and lattice configuration. We systematically measured dynamic aperture, tunes, and phase space trajectories for a large number of nominal and perturbed configurations. Our results show robustness of the system to perturbations in agreement with simulations, as well as the expected DA scaling with insert strength. Tune footprints are also consistent with simulations and previous results. Phase space reconstruction was improved significantly, with invariant jitter comparable to that predicted by simulations. Slightly better jitter is observed for the invariant as compared to regular actions, but analysis uncertainty is limited by the BPM systematics and noise. Based on these encouraging results, we plan to proceed with direct measurement of beam losses and stabilization with space charge dominated proton beams, for which the IOTA proton injector has just been commissioned.

REFERENCES

[1] D. Amorim *et al.*, "Single-beam transverse collective effects for HE-LHC", *ICFA Beam Dyn. Newslett.*, vol. 72, pp. 151–174, 2017.

[2] J. Gareyte, J. P. Koutchouk, and F. Ruggiero, "Landau Damping, Dynamic Aperture and Octupoles in LHC", LHC Project Report 91, 1997.

[3] V. Danilov and S. Nagaitsev, "Nonlinear accelerator lattices with one and two analytic invariants", *Phys. Rev. Spec. Top. Accel. Beams*, vol. 13, no. 8, p. 084002, Aug. 2010. doi:10.1103/PhysRevSTAB.13.084002

[4] S. Antipov *et al.*, "IOTA (Integrable Optics Test Accelerator): facility and experimental beam physics program", *J. Instrum.*, vol. 12, no. 03, T03002–T03002, Mar. 2017. doi:10.1088/1748-0221/12/03/T03002

[5] N. Kuklev, Y. K. Kim, S. Nagaitsev, AL. Romanov, and A. Valishev, "IOTA Run 2 Beam Dynamics Studies in Nonlinear Integrable Systems", in *Proc. IPAC'21*, Campinas, Brazil, May 2021, pp. 1964–1967. doi:10.18429/JACoW-IPAC2021-TUPAB228

[6] A. Valishev *et al.*, "First Results of the IOTA Ring Research at Fermilab", in *Proc. IPAC'21*, Campinas, Brazil, May 2021, pp. 19–24. doi:10.18429/JACoW-IPAC2021-MOXB02

[7] M. Henon and C. Heiles, "The applicability of the third integral of motion: Some numerical experiments", *Astron. J.*, vol. 69, p. 73, Feb. 1964. doi:10.1086/109234

[8] S. A. Antipov, S. Nagaitsev, and A. Valishev, "Single-particle dynamics in a nonlinear accelerator lattice: attaining a large tune spread with octupoles in IOTA", *J. Instrum.*, vol. 12, no. 04, pp. P04008–P04008, Apr. 2017. doi:10.1088/1748-0221/12/04/P04008

[9] J. Wieland *et al.*, "Measured dynamic aperture and detuning of nonlinear integrable optics", in *Proc. IPAC'24*, Nashville, TN, USA, May 2024, pp. 3019–3022. doi:10.18429/JACoW-IPAC2024-THPC21

[10] J. Wieland *et al.*, "Experimental measurements for extracting nonlinear invariants", in *Proc. IPAC'24*, Nashville, TN, USA, May 2024, pp. 3015–3018. doi:10.18429/JACoW-IPAC2024-THPC20

[11] S. S. Baturin, "Hamiltonian preserving nonlinear optics", *Physica D: Nonlinear Phenomena*, vol. 439, p. 133394, 2022. doi:10.1016/j.physd.2022.133394

[12] "Frequency Map Analysis and Particle Accelerators", in *Proc. PAC'03*, Portland, OR, USA, May 2003, pp. 378–382. doi:10.1109/PAC.2003.1288929

[13] N. Kuklev *et al.*, "Unified differentiable digital twin for the iota/fast facility", in *Proc. IPAC'25*, Taipei, Taiwan, Jun. 2025, pp. 2901–2904. doi:10.18429/JACoW-IPAC2025-THPM101

[14] R. E. Meller, "Decoherence of Kicked Beams", SSC-N-360, 1987. https://lss.fnal.gov/archive/other/ssc/ssc-n-360.pdf

[15] Z. Liu and M. Tegmark, "Machine learning conservation laws from trajectories", *Phys. Rev. Lett.*, vol. 126, no. 18, p. 180604, May 2021. doi:10.1103/PhysRevLett.126.180604